https://doi.org/10.1016/j.ijhydene.2017.05.075

Modeling of Direct Carbon Solid Oxide Fuel Cells with H_2O and CO_2 as gasification agents

Haoran Xu[1], Bin Chen[1], Houcheng Zhang[1,2], Qiong Sun[1], Guangming Yang[4], Meng Ni[1,3*]

[1] Building Energy Research Group, Department of Building and Real Estate The Hong Kong Polytechnic University, Hung Hom, Kowloon, Hong Kong, China

[2] Department of Microelectronic Science and Engineering, Ningbo University, Ningbo 315211, China

[3] Environmental Energy Research Group, Research Institute for Sustainable Urban Development (RISUD), The Hong Kong Polytechnic University, Hung Hom, Kowloon, Hong Kong, China

[4] Jiangsu National Synergetic Innovation Center for Advanced Materials (SICAM), College of Chemical Engineering, Nanjing Tech University, No.5 Xin Mofan Road, Nanjing 210009, P.R. China

Abstract:

In this paper, 2D models for direct carbon solid oxide fuel cells (DC-SOFCs) with H_2O and CO_2 as agents for carbon gasification are developed. The simulation results are compared with experimental data and good agreement is obtained. The performance of DC-SOFCs with two agents are compared at different operating potential, temperature and anode inlet gas flow rate. It is found that the H_2O assisted DC-SOFC performs significantly better than the CO_2-assisted DC-SOFC, indicating the suitability of H_2O for DC-SOFCs. It is also found that a higher temperature could greatly improve the performance of both kinds of DC-SOFCs. At a temperature of 1000K and operating voltage of 0.5V, the current density from the CO_2-assisted DC-SOFC is close to 0 while it is still above $1000 Am^{-2}$ from the H_2O-assisted DC-SOFC, indicating the possibility of operating the H_2O assisted DC-SOFC at reduced temperature. It is found that the anode gas flow rate does not significantly affect the performance of DC-SOFC. To further improve the performance of H_2O assisted DC-SOFCs, developing suitable catalysts

for enhancing carbon gasification kinetics could be a good strategy. The results of this study form a solid foundation to understand H_2O assisted DC-SOFCs.

Keywords: Solid oxide fuel cell (SOFC); Steam gasification of carbon; Mathematical modeling

* Corresponding author:
Email: bsmengni@polyu.edu.hk; Tel: 852-27664152; Fax: 852-27645131.

1. Introduction

Growing concern on energy crisis and environmental problems has driven worldwide research attention into clean and high efficiency energy technologies. Although the contribution from renewable solar and wind energy is increasing, fossil fuels are still the major energy source and will continue to be the dominating energy source for the coming decades. As the major component of fossil fuels, solid carbon fuels are widely used due to their low price. However, most solid carbon fuels are directly burned in coal-fired power plants for electricity generation with hazardous gases emission and low energy efficiency (typically < 40%). Clean and high efficiency technology for electricity generation using solid carbon fuels is therefore needed in the coming decades.

Solid oxide fuel cells (SOFCs) are potential power sources for clean and efficient conversion from fuels to electricity [1-8]. Unlike traditional power plant based on thermodynamic cycles, the SOFC directly converts a fuel's chemical energy into electricity via electrochemical reactions. This one-step process ensures a much higher energy conversion efficiency (>50%) than that of the coal-fired power plant. The emission gas from the SOFC can be easily collected and post-processed, enabling easy emission control. Therefore, SOFC can be a good alternative to traditional power plants for electricity generation using solid carbon fuels.

A typical SOFC has 3 layers: two porous electrodes and a dense electrolyte. Oxygen molecules are supplied to the cathode and are reduced at the triple phase boundary (TPB) in the porous cathode to O^{2-} ions, which subsequently transport through the electrolyte to the anode side.

Fuel molecules diffuse to the TPB in the anode and react with O^{2-} ions to release electrons, which transport to cathode through external circuit. These processes take place continuously as long as fuels and oxidants are continuously supplied to SOFC. Gaseous fuels such as H_2 and CO are usually used in SOFCs due to their fast transportation and high electrochemical reaction activity. However, gaseous fuels have much smaller energy density than that of liquid or solid fuels. In addition, solid fuels like coals are cheaper than gaseous fuels, which brings great benefits in decreasing overall cost and opening new markets. In order to utilize solid carbon in SOFCs, direct-carbon solid oxide fuel cells (DC-SOFCs) have been developed. Due to the large size of carbon particles and small pore size of DC-SOFC anode, carbon fuel is difficult to reach the anode TPB through the porous anode layer. Thus, it is now well accepted that the operation of DC-SOFC is based on the CO_2 shuttling mechanism: carbon is gasified by CO_2 (Boudouard reaction) to produce CO, which diffuses to the TPB and electrochemically oxidized to produce electrons and CO_2. The Boudouard reaction not only maintains a continuous supply of CO gas for electrochemical reaction, but also decreases CO_2 concentration in anode, which improves the local equilibrium potential and facilitates the electrochemical reaction kinetics.

Since Nakagawa and Ishida's first experimental study [9] , DC-SOFCs have received extensive research and been further developed. Based on the CO_2 shuttling mechanism, catalysts for enhancing Boudouard reaction kinetics have been developed to improve the performance of DC-SOFCs. Wu et al.[10] adopted Fe_mO_n-alkaline metal oxide catalyst for graphite and

activated carbon in DC-SOFCs and greatly enhanced CO formation rate was observed. Besides, they successfully obtained a peak power density of 286 mW cm^{-2} at 1123 K even without external CO_2 feeding. Li et al.[11] used Ni, K, Ca as catalyst in carbon black and found that the catalytic effects were: K>Ni>Ca. Tang et al.[12] used Fe as catalyst for DC-SOFCs and achieved a 10 hour operation lifetime before carbon power and catalyst were sintered. Alexander et al.[13] employed biomass char in SOFC and obtained a comparable performance with activated carbon. Yu et al.[14] used different kinds of carriers (CO_2 and Ar) in DC-SOFCs and found that the carrier gases had great effects on the performance of the cell. Jiao et al.[15] enlarged the specific surface area of the coal char fuel for DC-SOFC by treating coal char with alkali. The peak power density of DC-SOFCs was improved from 62 mW cm^{-2} for conventional coal char to 220 mW cm^{-2} for the alkali modified coal char. The use of CO_2 as a gasification agent has been demonstrated to be feasible for DC-SOFC. But the operating temperature of CO_2-assisted DC-SOFC is usually quite high, typically ≥1123K, due to the relatively low gasification kinetics even with catalyst. The high operating temperature limits the choice of materials for the interconnect and causes coarsening of catalyst particles in the long-term operation, which in turn causes high cost and poor durability of DC-SOFC.

In order to lower the operating temperature with good power output, alternative carbon gasification strategy is needed. As H_2O is usually used as an agent for coal gasification, it can be a good potential agent for DC-SOFC. Some preliminary analyses have been done on the use of H_2O as an agent for DC-SOFC. Lee et al.[16] thermodynamically compared these

two gasification agents. The thermodynamic model indicated that the addition of gasification agents (CO_2 or H_2O) did not considerably affect the DC-SOFC efficiency and power output. However, the effects of the gasification agent on the carbon gasification kinetics are not considered in their thermodynamic analyses. Since the performance of DC-SOFC is limited by the carbon gasification kinetics, the effect of using gasification agent should be significant. In a recent study, a 1D membrane-electrode-assembly (MEA) model was developed by Ong and Ghoniem [17] to study the indirect carbon fuel cell with H_2O gasification and CO_2 gasification. It was found that DC-SOFCs performed 3-5 times better with H_2O recycling from anode to the gasifier than with CO_2 between 700 ºC and 800 ºC. Their preliminary simulations form a good basis for understanding the difference between the H_2O gasification and CO_2 dry gasification. However, their model is 1D and only considers external carbon gasification for indirect carbon fuel cells.

The processes of internal carbon gasification in anode chamber for DC-SOFCs are different from those of a DC-SOFC with external gasification, as the counter diffusion processes of H_2/H_2O or CO/CO_2 pairs in the porous anode layer of the internally gasified DC-SOFC are highly coupled with the gasification processes and the electrochemical reactions. Besides, the internal chemical reactions could largely affect the overall cell performance as they provide the fuels for electrochemical reactions. The rate-determining step for DC-SOFC could be switched from electrochemical reaction to carbon gasification reaction. Therefore, there is a need to systematically investigate and compare the DC-SOFC with H_2O gasifying agent and that with

CO_2 gasifying agent.

In order to fill the research gap mentioned above, 2D mathematic models are developed for DC-SOFCs with H_2O or CO_2 as gasification agent (referred as H_2O-assisted and CO_2-assisted in the remaining part of the paper) in anode chamber. Detailed simulations are carried out in this paper to investigate its coupled transport and reaction processes. The models are validated by comparing the initial simulation results with experimental data and good agreement is observed.

2. Model description

2D mathematical models are developed to simulate the chemical/electrochemical reaction, ion/electron transport and mass/momentum transport in DC-SOFCs with CO_2 and H_2O as agents. The schematics of the CO_2 assisted DC-SOFC and H_2O assisted DC-SOFCs are shown in Fig.1. Solid carbon is placed in the anode chamber and H_2O (or CO_2) is also supplied to the anode. Solid carbon in anode chamber is very close to the porous anode. The surface area of button cell is 0.45 cm^2.The thickness of anode, electrolyte and cathode are 400μm, 8μm and 24μm, respectively. The modeled button cell uses Ni-YSZ composites (mixture of YSZ (yttrium stabilized zirconium) and nickel) as anode, bilayer YSZ/SDC electrolyte and LSCF (lanthanum strontium cobalt ferrite) as cathode. Material properties such as ionic and electronic conductivities are listed in Table 1. Widely used chemical and electrochemical reaction and other tuning parameters are adopted and listed in Table 2.

2.1 Model assumption

(1) In H_2O assisted DC-SOFCs, H_2 and CO both participate in the electrochemical reactions and share the TPB sites, which is proportional to their relative local concentration.

(2) Triple phase boundaries (TPBs) are distributed uniformly in the whole porous electrode. Both ionic- and electronic- conducting phases in the porous electrodes are homogeneous and continuous.

(3) Gases in the model (CO, H_2O, H_2, O_2, N_2) are ideal gases and incompressible gas flow in the gas channels.

(4) Temperature distribution in the cell is uniform due to its small size.

(5) The volume of carbon fuel in the anode chamber does not change with time.

2.2 Chemical reactions

In gasification driven DC-SOFCs, Boudouard reaction plays a key role as it produces CO to maintain the electrochemical reaction. This key reaction (Eq. (1)) converts carbon and CO_2 into CO. Here solid carbon is the energy source and CO is an energy carrier that transports the chemical energy from solid carbon to the anode TPB. The reaction rate of Boudouard reaction is calculated as Eq. (2)[18].

$$C + CO_2 \leftrightarrow 2CO \qquad (1)$$

$$R_{C\_CO2} = \frac{K_1 p_{CO_2}}{1 + K_2 p_{CO} + K_3 p_{CO_2}} \qquad (2)$$

When H_2O is added in DC-SOFCs, the main chemical reaction rate in anode chamber becomes water gasification reaction (Eq. (3)) instead of Boudouard reaction as water gasification has a

much higher reaction rate. The reaction rate of water gasification reaction is calculated as Eq. (4)[18]

$$C + H_2O \leftrightarrow CO + H_2 \qquad (3)$$

$$R_{C\_H2O} = \frac{K_4 p_{H_2O}}{1+K_5 p_{H_2}+K_6 p_{H_2O}} \qquad (4)$$

Besides, water gas shift reaction (WGSR) catalyzed by nickel in anode electrode also plays an important role as shown in Eq. (5). This reaction converts CO into H_2 and ensures H_2 to mainly participate in electrochemical reaction. The Reaction rate of WGSR is calculated by Eqs. (6-9) [19].

$$CO + H_2O \leftrightarrow CO_2 + H_2 \qquad (5)$$

$$R_{WGSR} = k_{sf}(p_{H_2O}p_{CO} - \frac{p_{H_2}p_{CO_2}}{K_{ps}}) \qquad (6)$$

$$k_{sf} = 0.0171\exp(\frac{-103191}{RT}) \text{ (mol m}^{-3}\text{ Pa}^{-2}\text{ s}^{-1}) \qquad (7)$$

$$K_{ps} = \exp(-0.2935Z^3 + 0.6351Z^2 + 4.1788Z + 0.3169) \qquad (8)$$

$$Z = \frac{1000}{T} - 1 \qquad (9)$$

Overall, in H_2O assisted DC-SOFCs, water gasification reaction becomes the key chemical reaction instead of Boudouard reaction. This change ensures a faster gas fuel supplement and brings in H_2 in the fuel cell. WGSR in anode electrode largely improves the percentage of H_2 component in gas fuel and makes H_2 as the main intermediate between solid fuel and anode electrode. Faster gas fuel production rate and better electrochemical reaction activity are thus achieved by introducing H_2O into DC-SOFCs.

2.3 Electrochemical reaction

In CO_2-assisted DC-SOFCs, CO is the only fuel to be electrochemically oxidized. While in H_2O-assisted DC-SOFCs, both H_2 and CO will be produced in chemical reactions and participate in the electrochemical reactions.

As air is supplied to the cathode of SOFC, O_2 molecules are reduced to form oxygen ions (O^{2-}) via Eq. (10)

$$O_2 + 4e^- \rightarrow 2O^{2-} \qquad (10)$$

The oxygen ions flow through the ionic-conducting electrolyte to the anode, where they react electrochemically with CO/H_2 molecules, form CO_2/H_2O and release electrons as shown in Eq. (11) and Eq. (12):

$$CO + O^{2-} \rightarrow CO_2 + 2e^- \qquad (11)$$

$$H_2 + O^{2-} \rightarrow H_2O + 2e^- \qquad (12)$$

The operating potential can be calculated by thermodynamic equilibrium potential and operating overpotential losses as shown in Eq. (13):

$$V = E_{eq} - \eta_{act} - \eta_{ohmic} \qquad (13)$$

The equilibrium potential (E_{eq}) is determined by the thermodynamic property of the reaction. In CO_2-assisted DC-SOFC, as only CO participate in the electrochemical reaction, the equilibrium potential can be calculated by the Nernst equation (Eq. 14-1).

However, for H_2O-assisted DC-SOFC, both H_2 and CO can participate in the electrochemical reaction. In the present study, the equilibrium potentials for CO fuel and H_2 fuel can be

determined by Eq. (14-1) and Eq. (14-2) respectively. It should be noted that the equilibrium potentials calculated by Eq. 14-1 and Eq. 14-2 are equal at an open circuit condition. When current is extracted from DC-SOFC, the equilibrium potentials for H_2 fuel and CO fuel become different due to the different overpotential losses involved in electrochemical oxidation of H_2 fuel and CO fuel.

$$E_{CO} = E_{CO}^0 + \frac{RT}{2F}\ln\left[\frac{P_{CO}^L (P_{O_2}^L)^{1/2}}{P_{CO_2}^L}\right] \qquad (14\text{-}1)$$

$$E_{H_2} = E_{H_2}^0 + \frac{RT}{2F}\ln\left[\frac{P_{H_2}^L (P_{O_2}^L)^{1/2}}{P_{H_2O}^L}\right] \qquad (14\text{-}2)$$

Here E^0 is the standard potential, R is the universal gas constant (8.3145 J mol^{-1} K^{-1}), T is the operating temperature (K), F is the Faraday constant (96485 C mol^{-1}). P^L is the local gas partial pressure. The value of E_{CO}^0 and $E_{H_2}^0$ can be calculated by Eq. (15) and Eq. (16) [19]:

$$E_{CO}^0 = 1.46713 - 0.0004527T \text{ (V)} \qquad (15)$$

$$E_{H_2}^0 = 1.253 - 0.00024516T \text{ (V)} \qquad (16)$$

The activation overpotential (η_{act}) is the potential barrier for the electrochemical reaction to overcome. Butler-Volmer equation is adopted to describe the relationship between the activation overpotential and the current density as shown in Eq. (17).

$$i = i_0\left\{\exp\left(\frac{\alpha n F \eta_{act}}{RT}\right) - \exp\left(\frac{(1-\alpha) n F \eta_{act}}{RT}\right)\right\} \qquad (17)$$

where α is the electron transfer coefficient, n is the number of transferred electrons per electrochemical reaction. i_0 is the exchange current density related to the fuel property and

electrode material. Considering temperature effect, i_0 can be further expressed as Eq. (18).

$$i_0 = \gamma \exp\left(-\frac{E_{act}}{RT}\right) \qquad (18)$$

where γ (Am^{-2}) is the pre-exponential factor and E_{act} is the activation energy level.

The ohmic overpotential (η_{ohmic}) is caused by ionic/electronic conduction. Thus it is related to the current intensity and ionic/electronic conductivity of the cell. η_{ohmic} can be calculated by Ohm law, more detailed information can be found in our previous work[20-22].

2.4 Mass transport

The rate of mass transport ($N_i, mol\, m^{-3}\, s^{-1}$) in channels and porous electrodes can be calculated by the general Fick's model as shown in Eq. (19)[23]:

$$N_i = -\frac{1}{RT}\left(\frac{B_0 y_i P}{\mu}\frac{\partial \mathrm{P}}{\partial \mathrm{z}} - D_i^{eff}\frac{\partial (y_i \mathrm{P})}{\partial \mathrm{z}}\right) \ (i = 1, \dots, n) \qquad (19)$$

where B_0 is the permeability of the porous electrodes, y_i is the mole fraction of component i, μ is the gas viscosity (N $m^{-1}s^{-1}$) and D_i^{eff} is the overall effective diffusion coefficient of component i (m^2s^{-1}), which can be further calculated by Eq. (20) for gas diffusion in the porous electrodes [24]:

$$D_i^{eff} = \frac{\varepsilon}{\tau}\left(\frac{1}{D_{im}^{eff}} + \frac{1}{D_{ik}^{eff}}\right)^{-1} \qquad (20)$$

where ε is the porosity, τ is the tortuosity factor, D_{ik}^{eff} and D_{im}^{eff} ($m^2\ s^{-1}$) are respectively the Knudsen diffusion coefficient and molecular diffusion coefficient. Detailed calculation of D_{im}^{eff} and D_{ik}^{eff} can be found in ref.[25]. It should be noted that only the molecular diffusion is considered in the gas channels as Knudsen diffusion becomes significant only when the mean-free path of the molecular species is comparable or larger than the pore size.

2.5 Fluid flow

The Navier-Stokes (N-S) equation including the Darcy's term is used to describe the momentum transport of gas species in porous electrodes as shown in Eq. (21):

$$\rho\frac{\partial u}{\partial t}+\rho u\nabla u=-\nabla p+\nabla[\mu\left(\nabla u+(\nabla u)^{T}\right)-\frac{2}{3}\mu\nabla u\Big]-\frac{\varepsilon\mu u}{k} \qquad (21)$$

where ρ (kg m^{-3}) is the gas density and u (m s^{-1}) is the velocity vector. When the last term on the right side is neglected, Eq. (20) is reduced to conventional N-S equation for momentum conservation in gas channels.

2.6 Model solution

Electric potentials are specified at two electrodes. Two ends of the cell are electrically insulated. Inflow gas mole fraction and flow rate (SCCM) are given at the channel inlets. The outflow condition is specified at the outlets of the gas channels. Zero flux is specified at the end of the electrodes and pressure condition is specified at the outlets of the two gas channels.

The model is solved at given operating conditions such as electric potentials, temperature, inlet gas flow rate and mole fraction. The output of the model includes distributions of the electrochemical reaction rates, chemical reaction rates and mole fraction of gas species in the cell. The commercial software COMSOL MULTIPHYSICS® is employed for the numerical simulation.

3 Results and discussion

3.1 Model validation

Single cells were prepared and tested for model validation of DC-SOFCs with both CO_2 and H_2O as agents. The fuel cell employed Ni-YSZ anode-supported anode, bilayer YSZ/SDC electrolyte and LSCF cathode. For the fuel cell test, the cell was sealed onto a quartz tube by means of silver paste and silver layers were printed onto the anode and cathode surfaces for current collection. The solid carbon was fixed by asbestos in the anode chamber. A quartz tube was positioned beneath the carbon layer for introducing CO_2 and H_2O. The inlet gas flow rate of anode was set as 30 SCCM (standard conditions). 10 SCCM H_2O was carried into anode by 20SCCM N_2 in the test. The operating temperature was kept constant at 850 $^{\circ}$C during the test. Current-voltage values were collected based on the four-terminal configuration. The schematic designs for fuel cell tests and other detailed information of the testing procedures could be found in ref.[10].

The modeling results of current-voltage characteristics for both CO_2-assisted DC-SOFCs and H_2O-assisted DC-SOFCs are compared with experimental data as shown in Fig. 2. The quite small difference between the modeling results and experimental data validates the present model. The same structure and tuning parameters are used in the subsequent parametric simulations.

3.2 Effect of applied voltage

The voltage-current density-power density curves of DC-SOFCs with two kinds of agents are

shown in Fig. 3. The detailed operating conditions are listed in Table 3.

It is found that the performance of DC-SOFCs with H_2O as agent is much higher than that with CO_2 as agent, which is consistent with the previous study[17]. For DC-SOFCs with H_2O as agent, the peak power density reaches 3852 W m^{-2} at 0.48V, which is more than two times of that with CO_2 as agent (1579 W m^{-2} at 0.44V).

This significantly higher performance of H_2O-assisted DC-SOFC is mainly caused by 2 factors. Firstly, faster carbon gasification kinetics by H_2O agent offers a higher mole fraction of fuel (both CO and H_2) and thus higher open circuit voltage. Secondly, with H_2 participating in electrochemical reaction together with CO, a much higher electrochemical reaction rate could be obtained in H_2O assisted DC-SOFCs. As can be seen from Fig. 4(a, b), the carbon gasification rate in H_2O assisted DC-SOFCs ranges from 6.45 mol m^{-3} s^{-1} to 20.7 mol m^{-3} s^{-1} at 1123 K and 0.5 V operating potential. While the carbon gasification rate in CO_2 assisted DC-SOFCs only ranges from 2.71 mol m^{-3} s^{-1} to 12.4 mol m^{-3} s^{-1}. Consequently, the fuel mole fraction (H_2 + CO) in H_2O assisted DC-SOFCs is much higher than that (CO) in CO_2 assisted DC-SOFCs at the same applied voltage as shown in Fig. 4(c, d) and thus the higher performance could be obtained.

3.3 Effect of anode inlet H_2O mole fraction

As H_2O is carried into anode by N_2 in the experiments, the anode inlet H_2O mole fraction only reaches about 33%, which is at a quite low level. Thus, it would be necessary to study the effect

of inlet H_2O mole fraction on the performance of DC-SOFC. The related operating conditions are listed in Table 4.

As can be seen in Fig. 5, the current density of DC-SOFC increases significantly with the increase of inlet H_2O mole fraction. The DC-SOFC only has a current density of 2000 Am^{-2} at 1% inlet H_2O mole fraction, while 7000 Am^{-2} is reached with 35% inlet H_2O mole fraction. With the further increase of inlet H_2O mole fraction, only a small increase of current density is achieved due to the limited steam carbon gasification reaction rate. This tendency is also indicated by the change of H_2/H_2O mole fraction ratio in anode. As shown in Fig. 6, the molar ratio of H2/H2O is quite small (<0.06) at 1% inlet H2O mole fraction, and it increases 2 more times (~0.2) at 35% inlet H2O mole fraction, which is almost at the same level with 99% inlet H2O mole fraction.

3.4 Effect of anode inlet gas flow rate

For H_2-fueled SOFCs, a higher anode inlet gas flow rate ensures a higher anode fuel concentration and higher current density at certain operating potential. For internal reforming SOFC, it is more complicated as the fuel (H_2 and CO) for electrochemical reaction is different from the hydrocarbon fuel. On the one hand, more hydrocarbon fuel may favor the internal reforming reaction, producing more H_2 and CO. On the other hand, high flowrate of the hydrocarbon fuel may also dilute the concentration of H_2 and CO fuel for electrochemical reaction if the reforming reaction is not high enough.

For DC-SOFCs with CO_2 as agent, the increase of anode inlet gas flow has a negative effect on its performance at an operating temperature of 1123K. As can be seen in Fig.7, with the anode inlet gas flow rate increasing from 1 SCCM to 30 SCCM, the current density of CO_2 assisted DC-SOFC decreases from 3500 A m^{-2} to 3100 A m^{-2}. This is mainly caused by relative slow Boudouard reaction rate, which has become the rate-determining step in DC-SOFCs. As a result, CO_2 produced by electrochemical reaction is already enough for carbon gasification at 1123K and the inlet CO_2 will only dilute the fuel in DC-SOFCs.

In H_2O assisted DC-SOFCs, the carbon gasification rate is faster and benefits more from the increase of anode inlet gas flow rate in the beginning. Until when the steam carbon gasification rate cannot catch up with the further increase of inlet gas flow rate, fuels in anode are also diluted by inlet H2O, which results in the decrease of the current density of DC-SOFC.

3.5 Effect of operating temperature

As can be seen from Fig.8, the current density of both H_2O-assisted DC-SOFC and CO_2 assisted DC-SOFC is increased at a higher temperature. For CO_2-assisted DC-SOFCs, with temperature increasing from 923 K to 1123 K, the current density is increased from 37 A m^{-2} to 3293 A m^{-2} when the temperature is increased from 923K to 1123K. This huge increase indicates that a relative higher temperature is very necessary for CO_2 assisted DC-SOFCs as Boudouard reaction rate is quite slow at a relatively lower temperature. For H_2O-assisted DC-SOFCs, the current density is 372 A m^{-2} at 923 K, which is almost 10 times of the current

density of CO_2-assisted DC-SOFCs. When the operating temperature reaches 1048 K, the current density of H_2O-assisted DC-SOFC reaches 3439 A m^{-2}, exceeding the current density of CO_2 assisted DC-SOFCs at 1123K. Finally, H_2O assisted DC-SOFCs achieves 7690 A m^{-2} at 1123 K, which is still more than 2 times higher than that of CO_2 assisted DC-SOFCs. Both H_2O and CO_2 assisted DC-SOFCs benefits from the increase of operating temperature. Apart from general improvement of electrochemical reaction kinetics as for most SOFCs, faster chemical reaction kinetics as a higher temperature also brings great benefits for DC-SOFCs.

It should also be noticed that H_2O assisted DC-SOFCs still has an acceptable output power density at relatively lower temperature. Thus, using H_2O as agent is very promising for DC-SOFCs at a wider range of temperature.

4 Conclusion

A multi-physics model is developed to study the performance of DC-SOFCs with H_2O and CO_2 as agents. Parametric analyses are carried out to investigate the effects of operating potential, anode inlet gas mole fraction/flowrate and operating temperature on the performance of DC-SOFCs. The performance of DC-SOFCs with two different agents are also compared to see the improvement by adding H_2O for carbon gasification in DC-SOFCs.

Benefiting from faster carbon gasification, H_2O-assisted DC-SOFCs has a much higher fuel concentration in anode than CO_2-assisted DC-SOFCs. Coupled with faster electrochemical reaction kinetics by H_2 fuel, using H_2O as agent significantly improves the performance of DC-

SOFCs compared with CO_2 agent. As can be seen from the Power-Voltage curve, H_2O-assisted DC-SOFC achieves a peak power density of 3852 W m^{-2}, which is more than 2 times higher than CO_2assisted DC-SOFCs. Besides, H_2O- assisted DC-SOFC has a much better potential for operating at wider temperature range due to its fast gasification reaction kinetics. It is also found that a high anode inlet gas flow rate is not necessary for DC-SOFCs.

Acknowledgement

This research is supported by a grant (PolyU 152127/14E) from Research Grant Council, University Grants Committee, Hong Kong SAR, and a grant from Environment and Conservation Fund (ECF 54/2015), Hong Kong SAR.

We gratefully acknowledge the financial support of the National Science Foundation of China (Grant No. 51406091).

Nomenclature

Abbreviation

CHP	Combined heat and power
DC-SOFC	Direct-carbon solid oxide fuel cell
LSM	Strontium-doped lanthanum manganite
SCCM	Standard cubic centime per minute
SOFC	Solid oxide fuel cell
TPB	Triple phase boundary
WGSR	Water gas shift reaction
YSZ	Yttrium stabilized zirconium

Roman

B_0	Permeability coefficient, m^2
c_{CO_2}	Molar concentration of carbon dioxide, $mol \cdot m^{-3}$
D_i^{eff}	Effective diffusivity of species i, $m^2 \cdot s^{-1}$

D_{ik}^{eff}	Knudsen diffusion coefficient of i , $m^2 \cdot s^{-1}$
D_{im}^{eff}	Molecular diffusion coefficient of i, $m^2 \cdot s^{-1}$
E_{acv}	Activation energy, $J \cdot mol^{-1}$
E_{CO}	Equilibrium potential for carbon monoxide oxidization, V
E_{CO}^0	Standard equilibrium potential for carbon monoxide oxidization, V
E_{eq}	Equilibrium Nernst potential, V
F	Faraday constant, 96485 $C \cdot mol^{-1}$
i_o	Exchange current density, $A \cdot m^{-2}$
n	Number of electrons transferred per electrochemical reaction
N_i	Flux of mass transport, $kg \cdot m^{-3} \cdot s^{-1}$
p	(partial) Pressure, Pa
R	Gas constant, 8.314 $J \cdot mol^{-1} \cdot K^{-1}$
R_{ce}	Reaction rate of Boudouard reaction, $mol \cdot m^{-3} \cdot s^{-1}$
T	Temperature, K
u	Velocity field, $m^3 \cdot s^{-1}$
V	Volume fraction
y_i	Molar fraction of component i

Greek letters

α	Charge transfer coefficient
β_{H_2}	Electrochemical kinetics parameter for H_2
ε	Porosity
η_{act}	Activation polarization, V
η_{ohmic}	Ohmic polarization, V
κ	Permeability, m^2
λ	Thermal conductivity, $W \cdot m^{-1} K^{-1}$

μ	Dynamic viscosity of fluid, Pa·s
ρ	Fluid density, $kg \cdot m^{-3}$
σ	Conductivity, S/m
τ	Tortuosity
$\emptyset$	Potential, V

Subscripts

an	Anode
ca	Cathode
co	Carbon monoxide
H_2	Hydrogen
l	Ionic phase
s	Electronic phase

Superscripts

0	Parameter at equilibrium conditions

eff	Effective
L	Local

Reference

[1] Gür TM. Comprehensive review of methane conversion in solid oxide fuel cells: Prospects for efficient electricity generation from natural gas. Progress in Energy and Combustion Science. 2016;54:1-64.

[2] Ni M. Modeling of solid oxide fuel cells. Science Bulletin. 2016; 61(17): 1311-1312.

[3] Lei L, Wang Y, Fang S, Ren C, Liu T, Chen F. Efficient syngas generation for electricity storage through carbon gasification assisted solid oxide co-electrolysis. Applied Energy. 2016;173:52-8.

[4] Zhu H, Kee RJ. Thermodynamics of SOFC efficiency and fuel utilization as functions of fuel mixtures and operating conditions. J Power Sources. 2006;161:957-64.

[5] Ni M, Leung DYC, Leung MKH. Electrochemical modeling and parametric study of methane fed solid oxide fuel cells. Energ Convers Manage. 2009;50:268-78.

[6] Zheng KQ, Ni M. Reconstruction of solid oxide fuel cell electrode microstructure and analysis of its effective conductivity. Science Bulletin. 2016; 61(1): 78-85.

[7] Shi Y, Li C, Cai N. Experimental characterization and mechanistic modeling of carbon monoxide fueled solid oxide fuel cell. J Power Sources. 2011;196:5526-37.

[8] Giddey S, Badwal SPS, Kulkarni A, Munnings C. A comprehensive review of direct carbon fuel cell technology. Progress in Energy and Combustion Science. 2012;38:360-99.

[9] Nakagawa N, Ishida M. Performance of an internal direct-oxidation carbon fuel cell and its evaluation by graphic exergy analysis. Industrial & Engineering Chemistry Research. 1988;27:1181-5.

[10] Wu Y, Su C, Zhang C, Ran R, Shao Z. A new carbon fuel cell with high power output by integrating with in situ catalytic reverse Boudouard reaction. Electrochemistry Communications. 2009;11:1265-8.

[11] Li C, Shi Y, Cai N. Performance improvement of direct carbon fuel cell by introducing catalytic gasification process. J Power Sources. 2010;195:4660-6.

[12] Tang Y, Liu J. Effect of anode and Boudouard reaction catalysts on the performance of direct carbon solid oxide fuel cells. Int J Hydrogen Energ. 2010;35:11188-93.

[13] Alexander BR, Mitchell RE, Gür TM. Experimental and Modeling Study of Biomass Conversion in a Solid Carbon Fuel Cell. J Electrochem Soc. 2012;159:B347-B54.

[14] Yu X, Shi Y, Wang H, Cai N, Li C, Tomov RI, et al. Experimental characterization and elementary reaction modeling of solid oxide electrolyte direct carbon fuel cell. J Power Sources. 2013;243:159-71.

[15] Jiao Y, Zhao J, An W, Zhang L, Sha Y, Yang G, et al. Structurally modified coal char as a fuel for solid oxide-based carbon fuel cells with improved performance. J Power Sources. 2015;288:106-14.

[16] Lee AC, Mitchell RE, Gür TM. Thermodynamic analysis of gasification-driven direct carbon fuel cells. J Power Sources. 2009;194:774-85.

[17] Ong KM, Ghoniem AF. Modeling of indirect carbon fuel cell systems with steam and dry gasification. J Power Sources. 2016;313:51-64.

[18] Huang Z, Zhang J, Zhao Y, Zhang H, Yue G, Suda T, et al. Kinetic studies of char gasification by steam and CO2 in the presence of H2 and CO. Fuel Processing Technology. 2010;91:843-7.

[19] Ni M. Modeling of SOFC running on partially pre-reformed gas mixture. Int J Hydrogen Energ. 2012;37:1731-45.

[20] Xu H, Chen B, Liu J, Ni M. Modeling of direct carbon solid oxide fuel cell for CO and electricity cogeneration. Applied Energy. 2016;178:353-62.

[21] Xu H, Chen B, Ni M. Modeling of Direct Carbon-Assisted Solid Oxide Electrolysis Cell (SOEC) for Syngas Production at Two Different Electrodes. J Electrochem Soc. 2016;163:F3029-F35.

[22] Xu H, Chen B, Irvine J, Ni M. Modeling of CH4-assisted SOEC for H2O/CO2 co-electrolysis. Int J Hydrogen Energ. 2016;41:21839-49.

[23] Suwanwarangkul R, Croiset E, Fowler MW, Douglas PL, Entchev E, Douglas MA. Performance comparison of Fick's, dusty-gas and Stefan–Maxwell models to predict the concentration overpotential of a SOFC anode. J Power Sources. 2003;122:9-18.

[24] Chan SH, Khor KA, Xia ZT. A complete polarization model of a solid oxide fuel cell and its sensitivity to the change of cell component thickness. Journal of Power Sources. 2001;93:130-40.

[25] Todd B, Young JB. Thermodynamic and transport properties of gases for use in solid oxide fuel cell modelling. J Power Sources. 2002;110:186-200.

[26] Shi Y, Cai N, Li C, Bao C, Croiset E, Qian J, et al. Modeling of an anode-supported Ni–YSZ|Ni–ScSZ|ScSZ|LSM–ScSZ multiple layers SOFC cell: Part I. Experiments, model development and validation. J Power Sources. 2007;172:235-45.

[27] Luo Y, Shi Y, Li W, Cai N. Comprehensive modeling of tubular solid oxide electrolysis cell for co-electrolysis of steam and carbon dioxide. Energy. 2014;70:420-34.

[28] Eguchi K. Ceramic materials containing rare earth oxides for solid oxide fuel cell. J Alloy Compd. 1997;250:486-91.

[29] Fan B, Yan J, Yan X. The ionic conductivity, thermal expansion behavior, and chemical compatibility of La0.54Sr0.44Co0.2Fe0.8O3-δ as SOFC cathode material. Solid State Sciences. 2011;13:1835-9.

[30] Tai LW, Nasrallah MM, Anderson HU, Sparlin DM, Sehlin SR. Structure and electrical properties of La1 − xSrxCo1 − yFeyO3. Part 2. The system La1 − xSrxCo0.2Fe0.8O3. Solid State Ionics. 1995;76:273-83.

List of Tables

Table 1 Material properties[26-30]

Parameters	**Value or expression**	**Unit**
Ionic conductivity		
YSZ	$3.34 \times 10^4 e^{\frac{-10300}{T}}$	Sm^{-1}
SDC	$\frac{100}{T} \times 10^{5.48077-\frac{3792.53}{T}}$	Sm^{-1}
LSCF	$\frac{100}{T} \times 10^{2.51289-\frac{3036.75}{T}}$	
Electronic conductivity		
LSCF	$\frac{100}{T} \times 10^{4.32576+\frac{1204.26}{T}}$	Sm^{-1}
Ni	$3.27 \times 10^6 - 1065.3T$	Sm^{-1}
Porosity		
Cathode	0.2	
Anode	0.6	
Anode volume fraction		
YSZ	0.4	
Ni	0.6	
S_{TPB}		
Cathode layer	2.14×10^5	m^2m^{-3}
Anode layer	2.14×10^5	m^2m^{-3}
Electrode tortuosity	3	

Table 2 Reaction parameters

Parameter	**Value**	**Unit**
Chemical reaction		
$\boldsymbol{K_1}$	9.32×10^{-4}	s mol kg^{-1} m^{-2}
$\boldsymbol{K_2}$	1.25×10^{-3}	Pa^{-1}
$\boldsymbol{K_3}$	3.82×10^{-5}	Pa^{-1}
$\boldsymbol{K_4}$	2.19×10^{-3}	s mol kg^{-1} m^{-2}
$\boldsymbol{K_5}$	9.88×10^{-4}	Pa^{-1}
$\boldsymbol{K_6}$	8.13×10^{-5}	Pa^{-1}
Electrochemical reaction		
γ_{H_2}	2.944×10^{10}	A m^{-2}
E_{act,H_2}	1.2×10^{5}	J mol^{-1}
γ_{O_2}	1.39×10^{9}	A m^{-2}
E_{act,O_2}	1.2×10^{5}	J mol^{-1}
γ_{CO}	1.673×10^{9}	A m^{-2}
$E_{act,CO}$	1.2×10^{5}	J mol^{-1}
α_{H_2}	0.75	
α_{CO}	0.5	

Table 3 Operation parameters for operating potential effect study in DC-SOFCs

Parameter	**Value**	**Unit**
Operating potential	0 – 0.8	V
Anode inlet gas flow rate	30	SCCM
Cathode inlet gas flow rate	10	SCCM
Anode gas composition for H_2O assisted DC-SOFC	H_2O 100%	
Cathode gas composition	Air	
Temperature	1123	K

Table 4 Operation parameters for anode inlet H_2O mole fraction effect study in DC-SOFCs

Parameter	**Value**	**Unit**
Operating potential	0.5	V
Anode inlet gas flow rate	30	SCCM
Cathode inlet gas flow rate	10	SCCM
Anode gas composition for H_2O assisted DC-SOFC	1% - 99%	
Cathode gas composition	Air	
Temperature	1123	K

Table 5 Operation parameters for anode inlet gas flow rate effect study in DC-SOFCs

Parameter	**Value**	**Unit**
Operating potential	0.5	V
Anode inlet gas flow rate	1 -30	SCCM
Cathode inlet gas flow rate	10	SCCM
Anode gas composition for H_2O assisted DC-SOFC	100%	
Cathode gas composition	Air	
Temperature	1123	K

Table 6 Operation parameters for temperature effect study in DC-SOFCs

Parameter	**Value**	**Unit**
Operating potential	0.5	V
Anode inlet gas flow rate	10	SCCM
Cathode inlet gas flow rate	10	SCCM
Anode gas composition for H_2O assisted DC-SOFC	100%	
Cathode gas composition	Air	
Temperature	923 - 1123	K

List of Figures

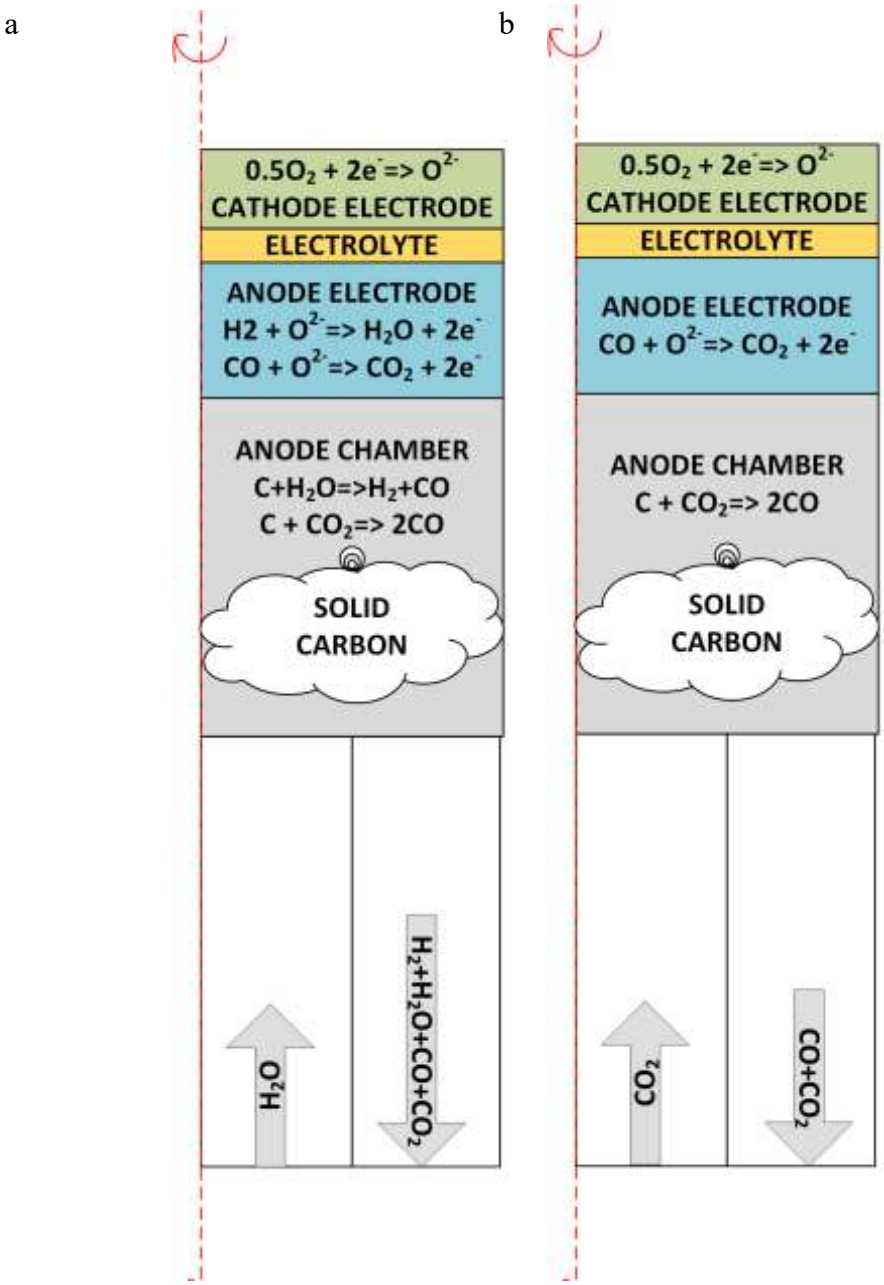

Fig.1. Schematic of H_2O assisted DC-SOFC(a) and CO_2 assisted DC-SOFC (b).

a

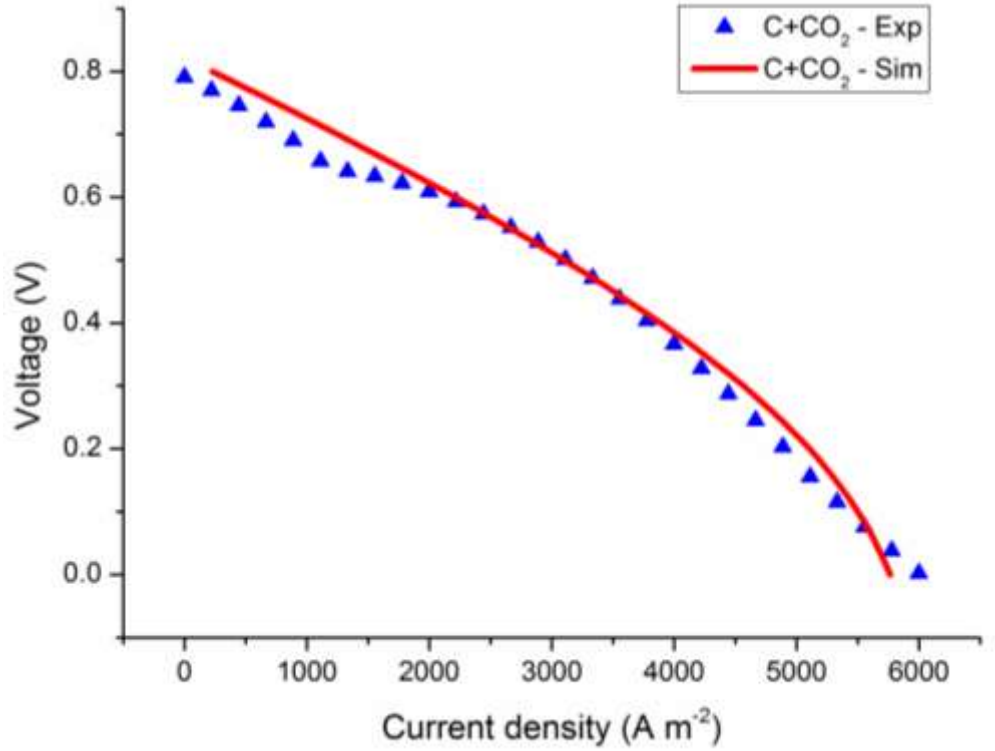

b

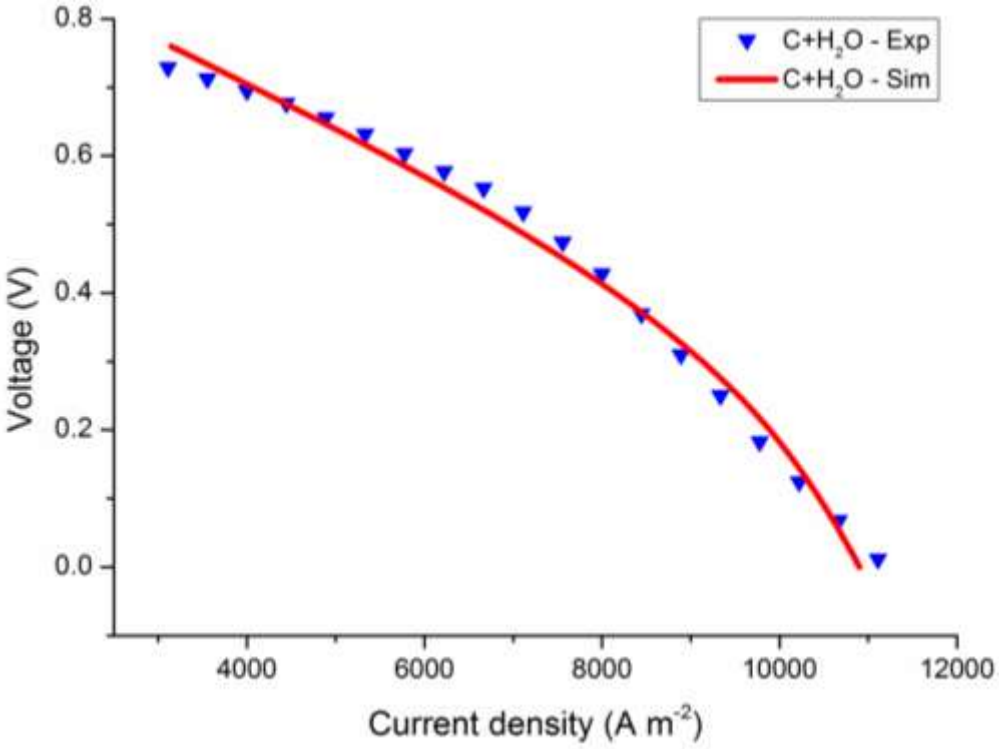

Fig.2 Model validation for DC-SOFCs with CO_2(a) and H_2O(b) as agents.

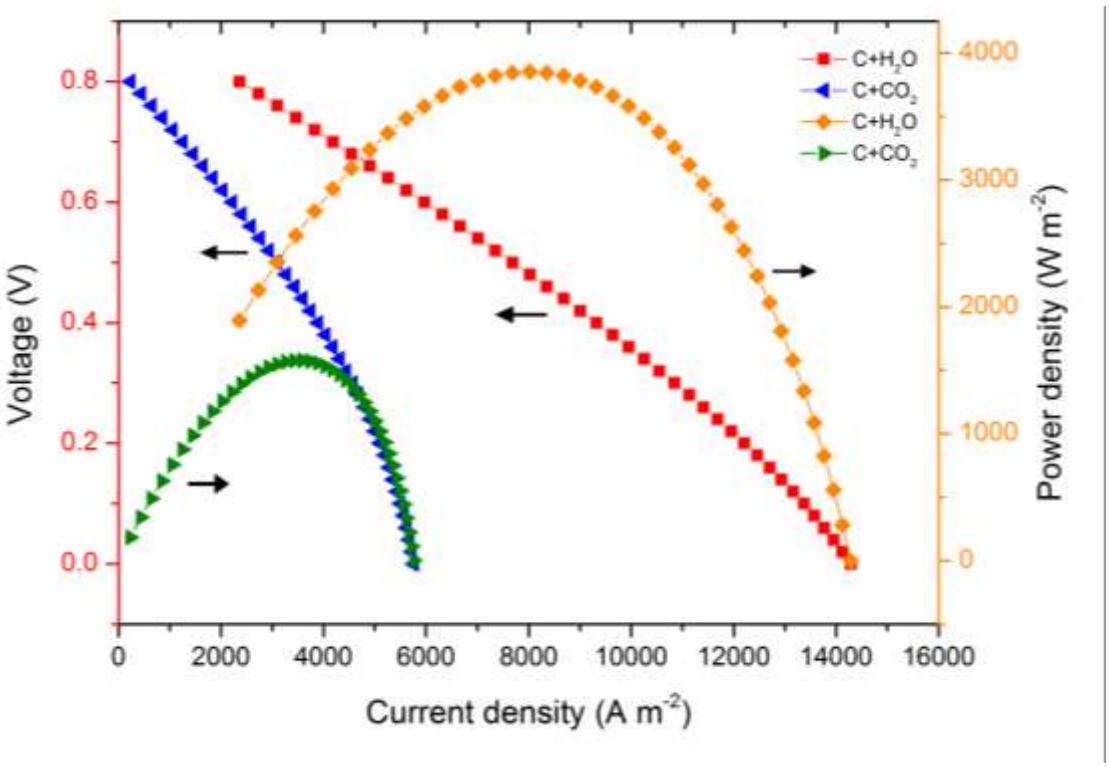

Fig. 3 The voltage-current density-power density relationships of DC-SOFCs with CO_2 and H_2O as agents

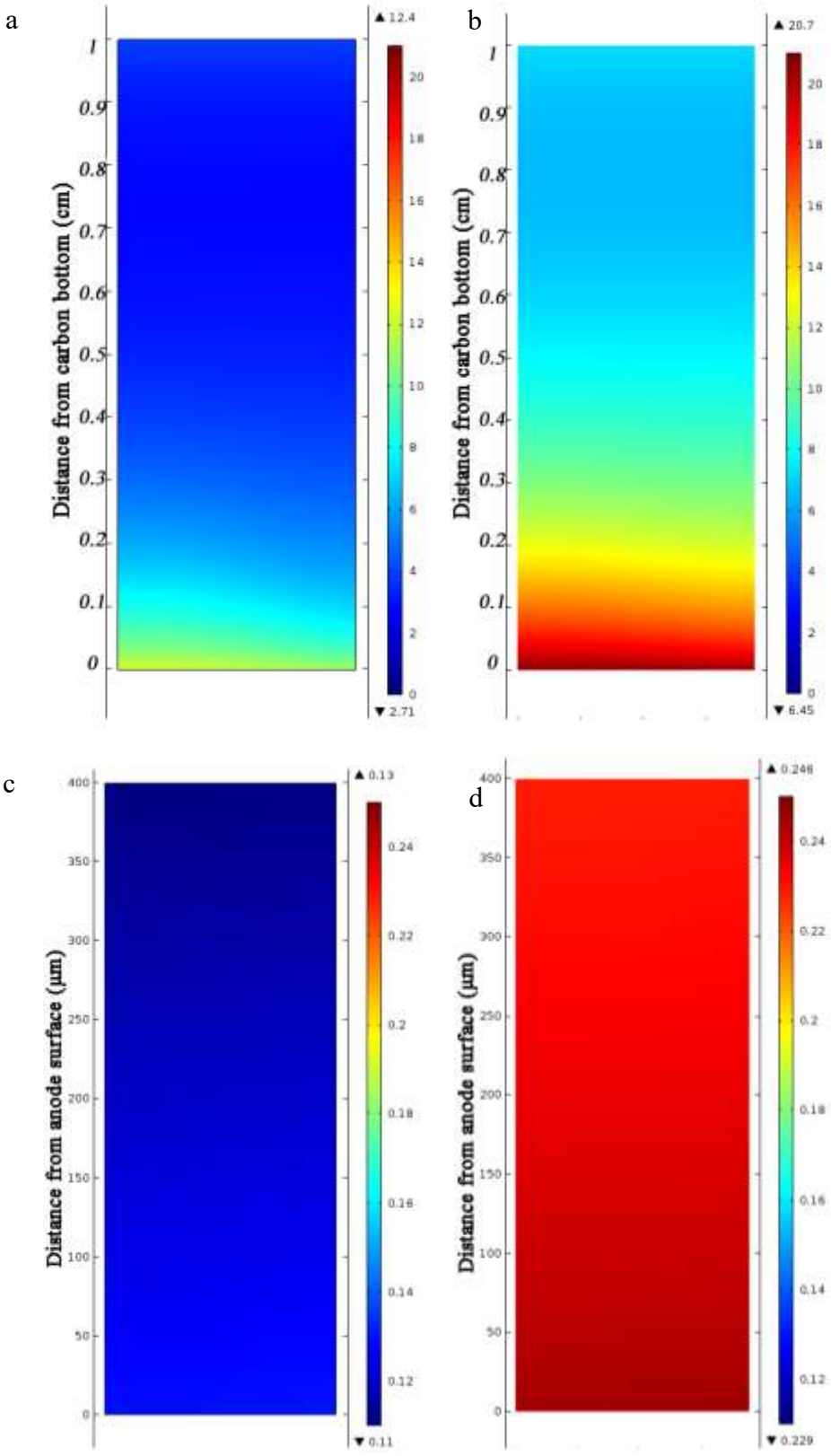

Fig. 4 The carbon gasification rate with CO_2 (a) and H_2O (b) as agents in carbon layer and mole fraction of fuel with CO_2 (c) and H_2O (d) in anode of DC-SOFCs at 0.5 V and 1123 K

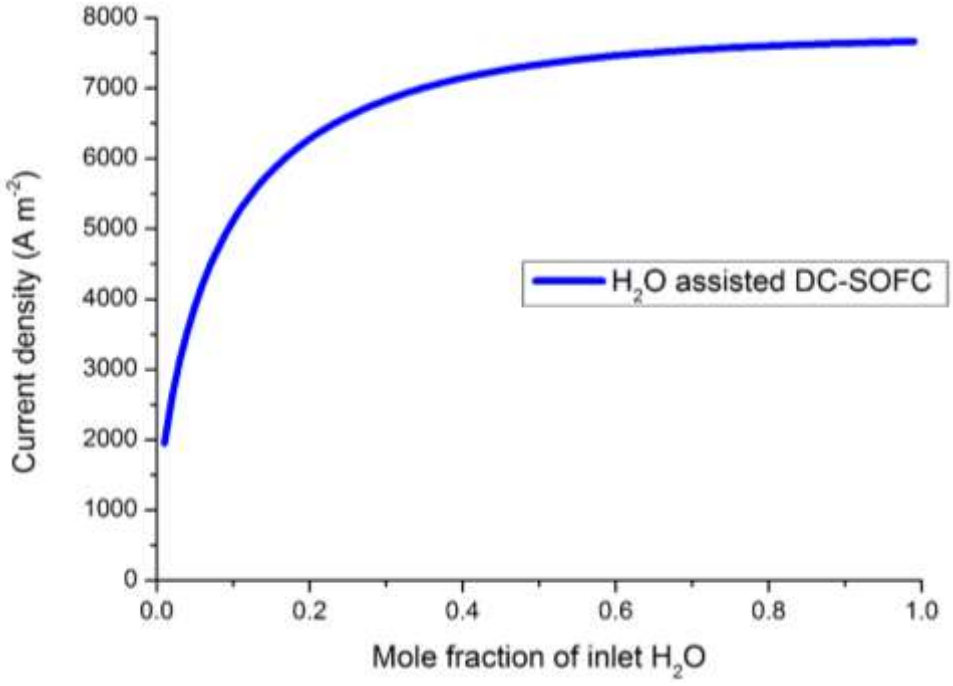

Fig. 5 Effect of inlet H_2O mole fraction change on the performance of DC-SOFC at 0.5V operating potential

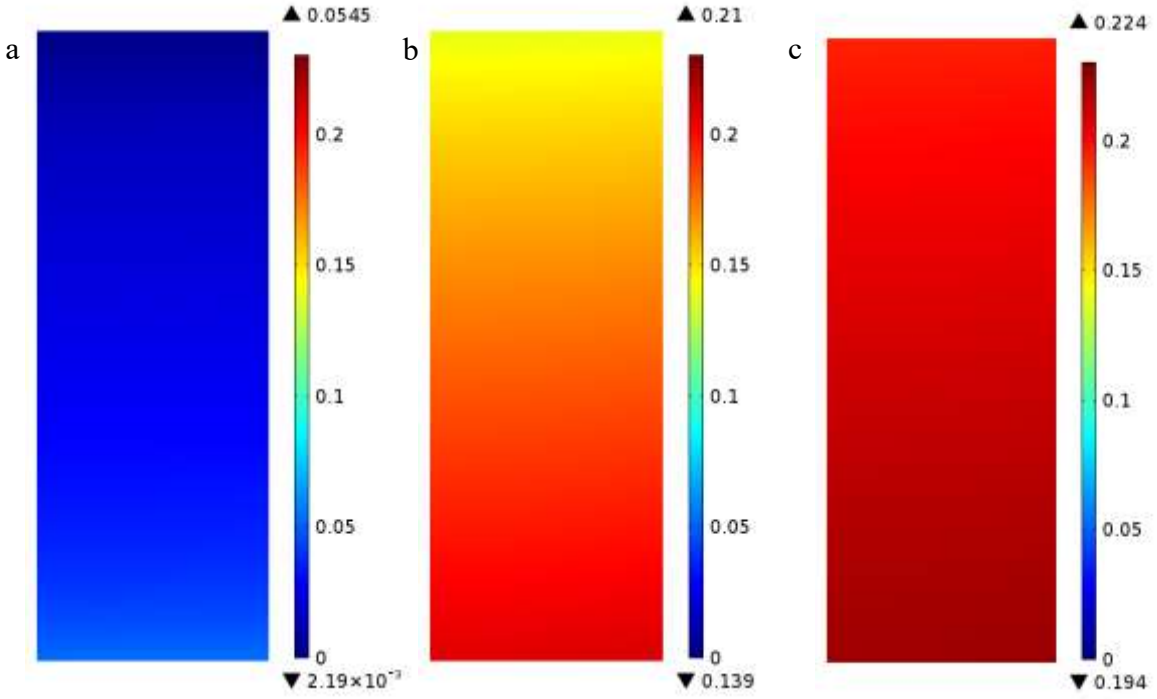

Fig. 6 Molar ratios of H2/H2O in the anode of DC-SOFCs with 1%(a), 35%(b) and 99%(c) mole fraction of H_2O in anode inlet gas

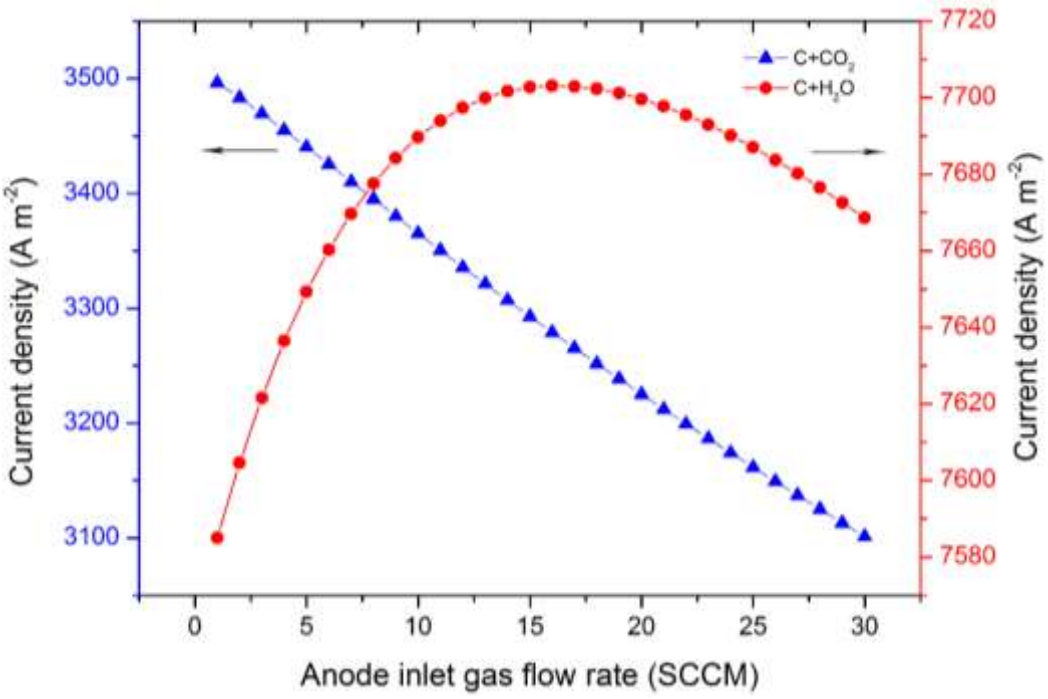

Fig. 7 The effect of anode inlet gas flow rate on current density of DC-SOFCs with CO_2 and H_2O as agents at 0.5 V and 1123 K

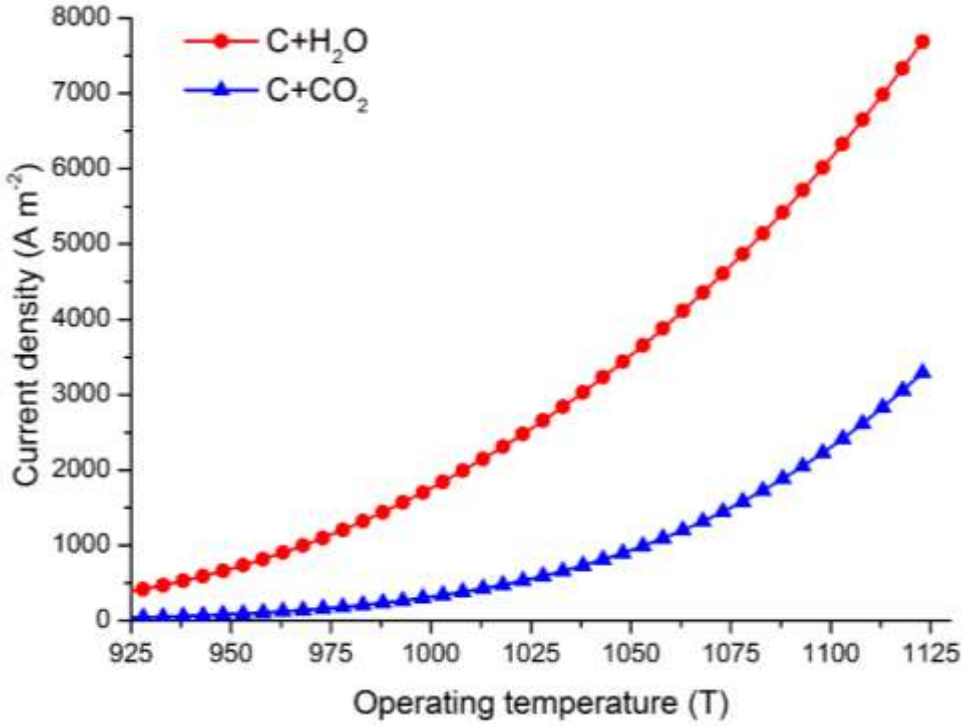

Fig.8 The effect of operating temperature on current density of DC-SOFCs with H_2O and CO_2 as agents at 0.5 V operating potential